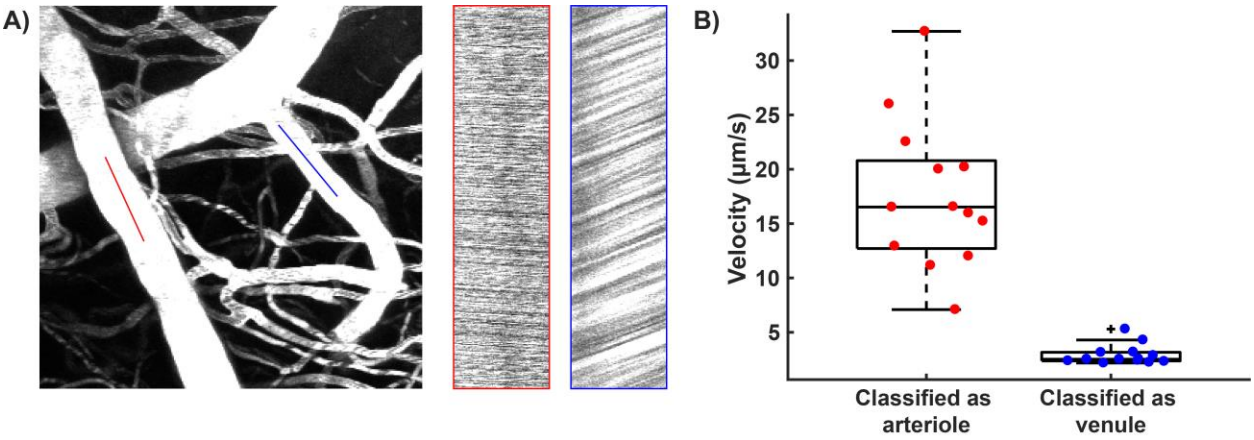

Supplementary figure 1: Confirmation of classification of arterioles. *Initial classification of vessels as arterioles was performed during the first imaging session for every mouse (n = 7), based on morphology and whether the vessel showed spontaneous diameter changes. To confirm our initial identification, line scans were acquired in 13 of 14 vessels that were classified as arterioles in cohort 1, to verify that they indeed have higher red blood cell (RBC) velocities than venules. The left panel in A) shows an example of a maximum intensity projection (MIP) acquired around one of the 14 vessels in cohort 1, indicated with the red line. The vessel in the field of view with the blue line did not show spontaneous diameter changes and was thus classified as a venule. The middle and the right panels in A) show kymographs acquired at the locations indicated with the red and blue lines in the left panel, respectively. The streaks in the kymographs represent moving RBCs surrounded by fluorescently labeled plasma. The slope of the streaks indicates the RBC velocity, with the steeper slope in the right kymograph indicating slower RBC velocity. B) shows the calculated RBC velocities in all 13 vessels that were classified as arterioles in which line scans were acquired, and in 13 nearby vessels that were classified as venules. All venular RBC velocities were lower than all arteriolar RBC velocities, confirming our initial classification.*

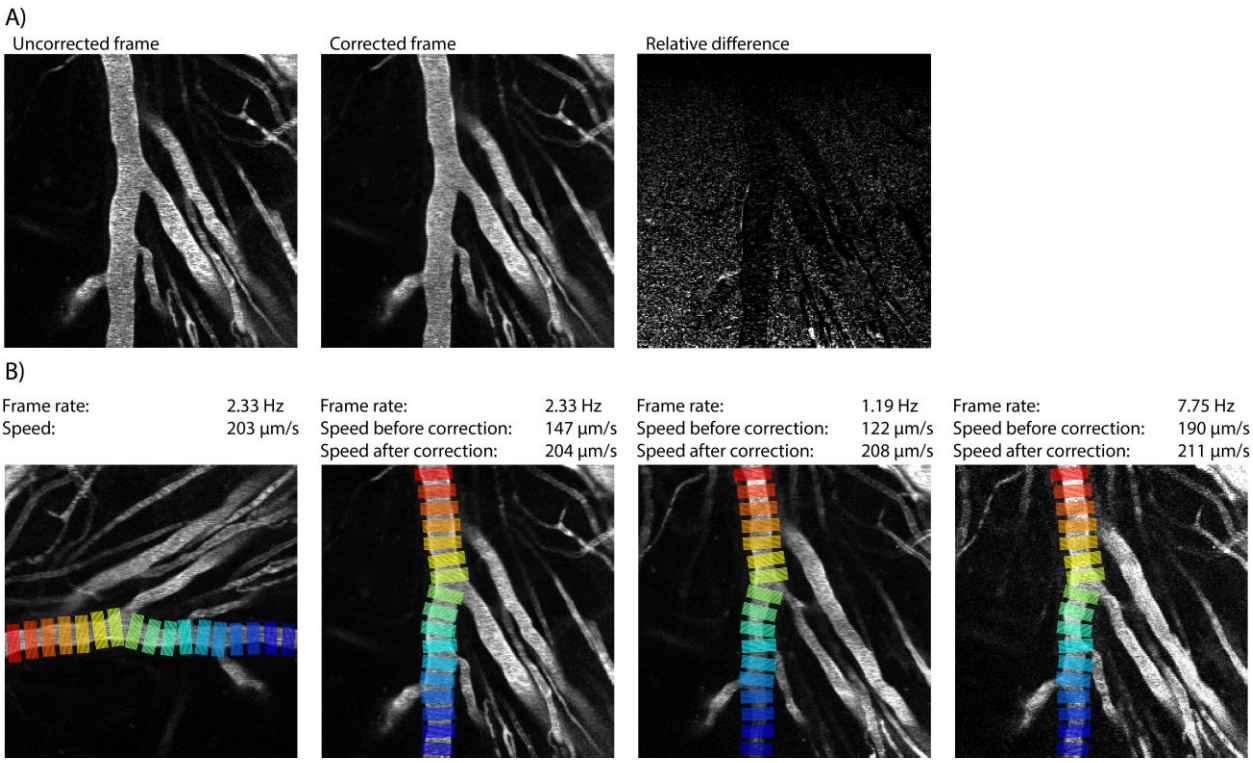

Supplementary figure 2: Validation of the pixel timing correction. *A) shows on the left the second image of a time lapse in which a cortical arteriole was imaged. In the middle, the same arteriole is shown, after applying the pixel timing correction, using the first and second image from the same time-lapse. On the right, the difference between the two images is shown. Note the increase in pixel difference intensities when you move down to the bottom of the subtracted image. B) shows the same arteriole, imaged in different orientations and at different imaging speeds. In the image on the left, the orientation is such that within the ROIs, the pixel acquisition times are nearly equal (the laser focal point moved line-by-line from top to bottom in the image), thus minimizing the bias on the wave speed calculation. The three images on the right are oriented such that the pixel acquisition times are maximally different within the ROIs, thus maximizing the bias on the wave speed calculation. The framerate of the second image is 2.33 Hz, equal to the framerate in the rest of this manuscript. The framerates of the third and fourth images are roughly twice slower and three times faster than that (note that for the fastest imaging, bidirectional scanning mode had to be applied). As expected, the slower the imaging, the more bias on the wave speed calculation (e.g., the wave at the slowest framerate was estimated to be 122 µm/s, versus 203 µm/s without any bias). However, after applying the pixel timing correction, all wave speeds were roughly equal.*

↓Supplementary figure 3: Three examples of the cross-correlation analysis pipeline to measure propagation of vessel diameter changes. *In the first two examples, significant vasomotion propagation was observed, and in the last example no propagation was observed. The left columns show visual stimulation datasets (at 0.06 Hz, 0.12 Hz and 0.06 Hz for the three examples respectively), and the right columns resting state datasets. The first row on each example shows the first image of the time-lapse with rainbow-colored regions of interest (ROIs) from where the diameter time-profiles were retrieved. The second row shows the raw diameter time-profiles; the third row shows normalized, detrended, and low-pass filtered (Norm. Detr. Filt.) time-profiles; the fourth row shows cross-correlation of all the curves in the fourth column with the reference ROI (the first blue ROI); the fifth row shows a linear correlation between the distance along the vessel versus the peaks in the retrieved cross-correlation curves. Note that in the first example, there is one noisy diameter time-profile (blue trace with lower diameter) in the visual stimulation data, which is dimmed in the Norm. Detr. Filt. data.*

Example 1

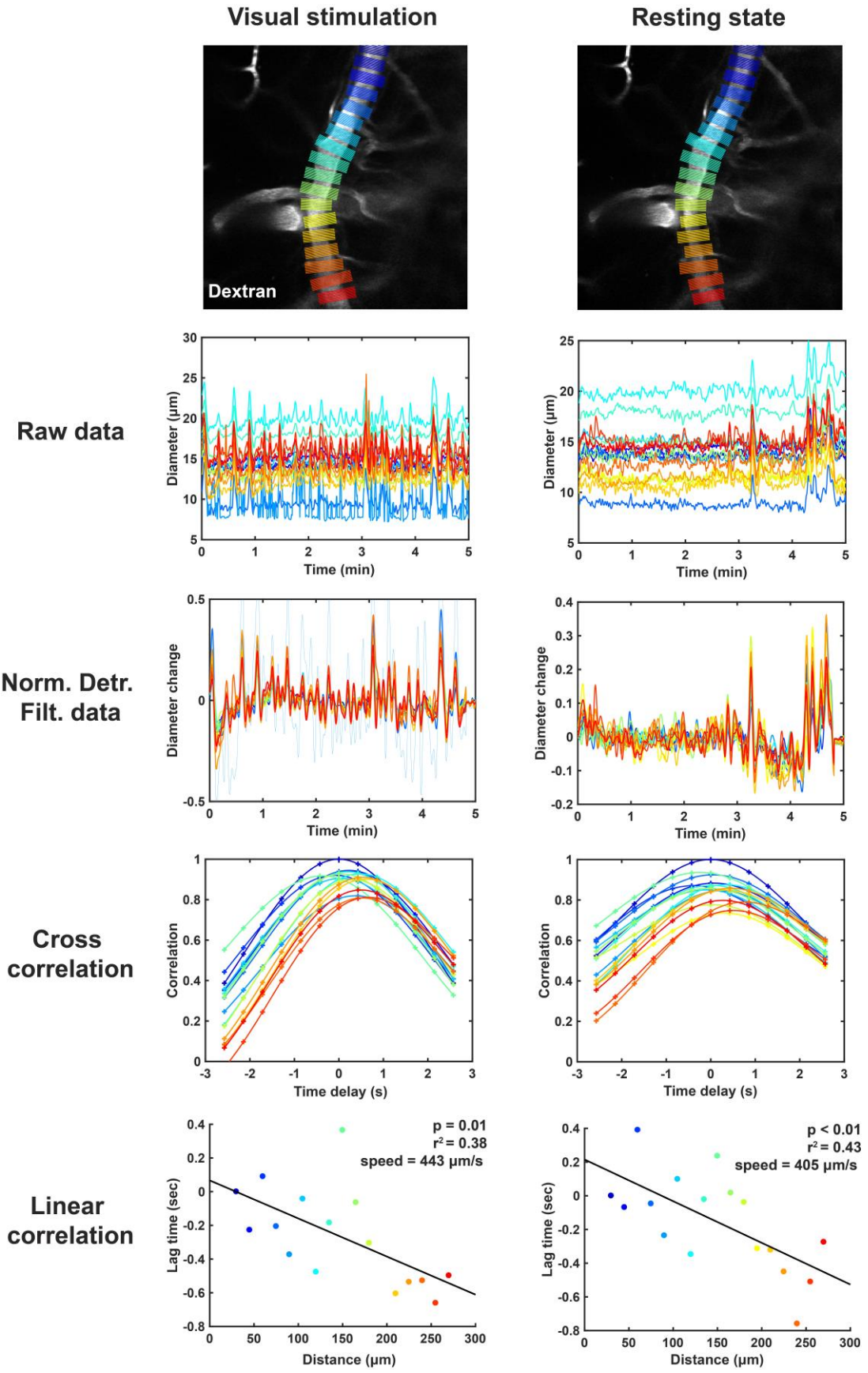
Visual stimulation
Resting state
Dextran
Raw data
Norm. Detr. Filt. data
Cross correlation
Linear correlation
Diameter (µm)
Time (min)
Diameter change
Correlation
Time delay (s)
Lag time (sec)
Distance (µm)
p = 0.01
r² = 0.38
speed = 443 µm/s
p < 0.01
r² = 0.43
speed = 405 µm/s

Example 2

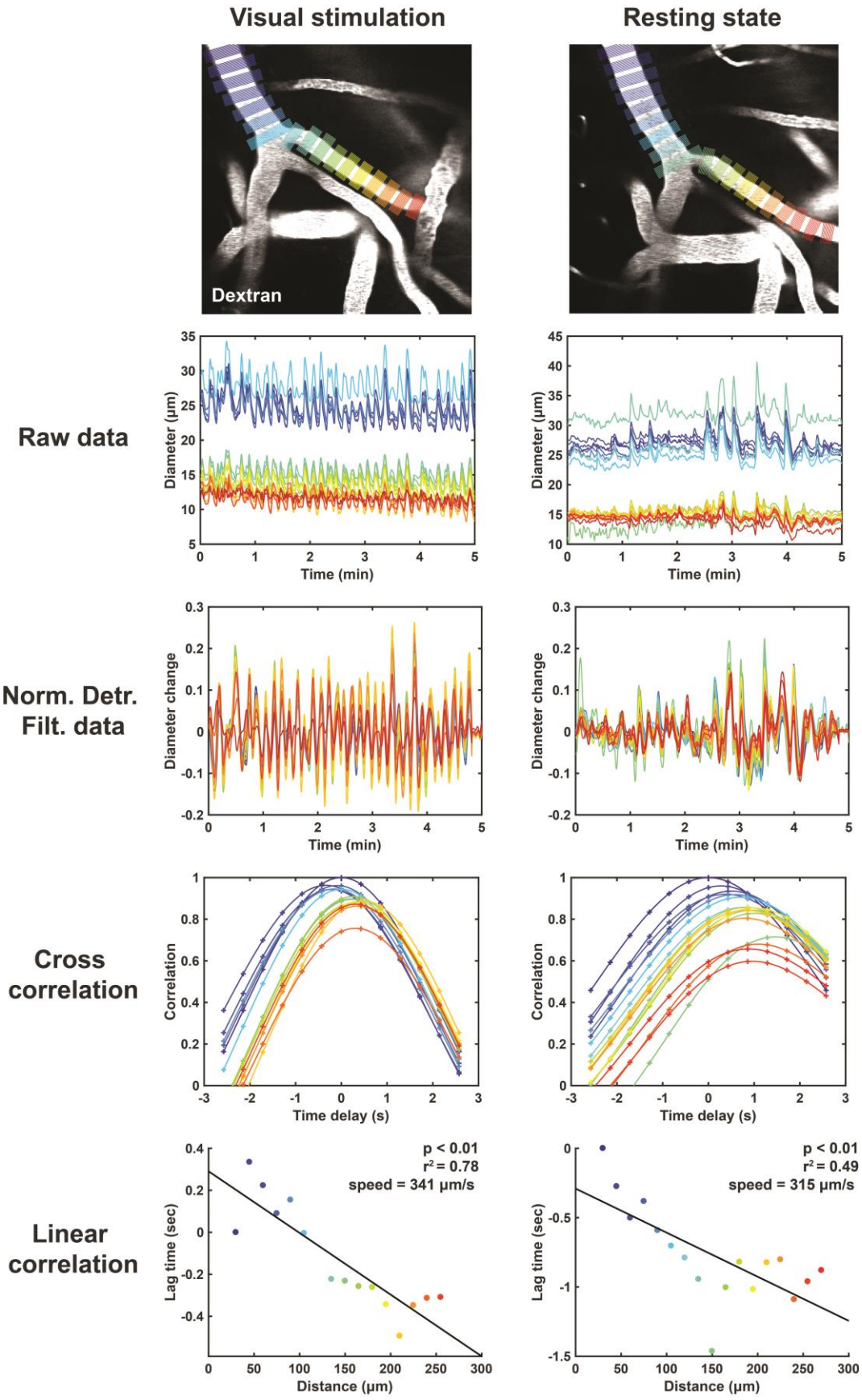
Visual stimulation
Resting state
Dextran
Raw data
Norm. Detr. Filt. data
Cross correlation
Linear correlation
Diameter (µm)
Time (min)
Diameter change
Correlation
Time delay (s)
Lag time (sec)
Distance (µm)
p < 0.01
r² = 0.78
speed = 341 µm/s
p < 0.01
r² = 0.49
speed = 315 µm/s

Example 3

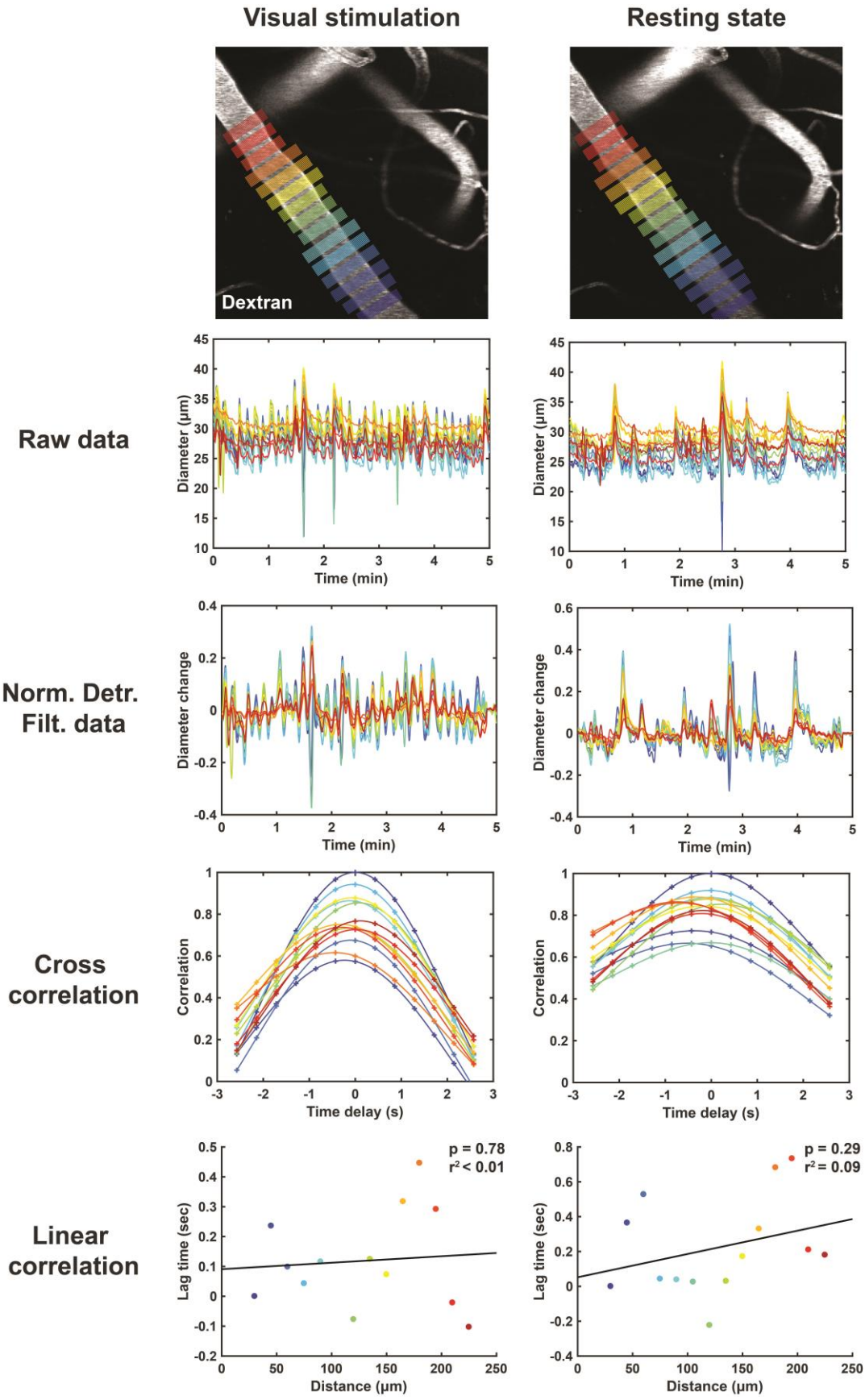
Visual stimulation
Resting state
Dextran
Raw data
Norm. Detr. Filt. data
Cross correlation
Linear correlation
Diameter (µm)
Time (min)
Diameter change
Correlation
Time delay (s)
Lag time (sec)
Distance (µm)
p = 0.78
r² < 0.01
p = 0.29
r² = 0.09

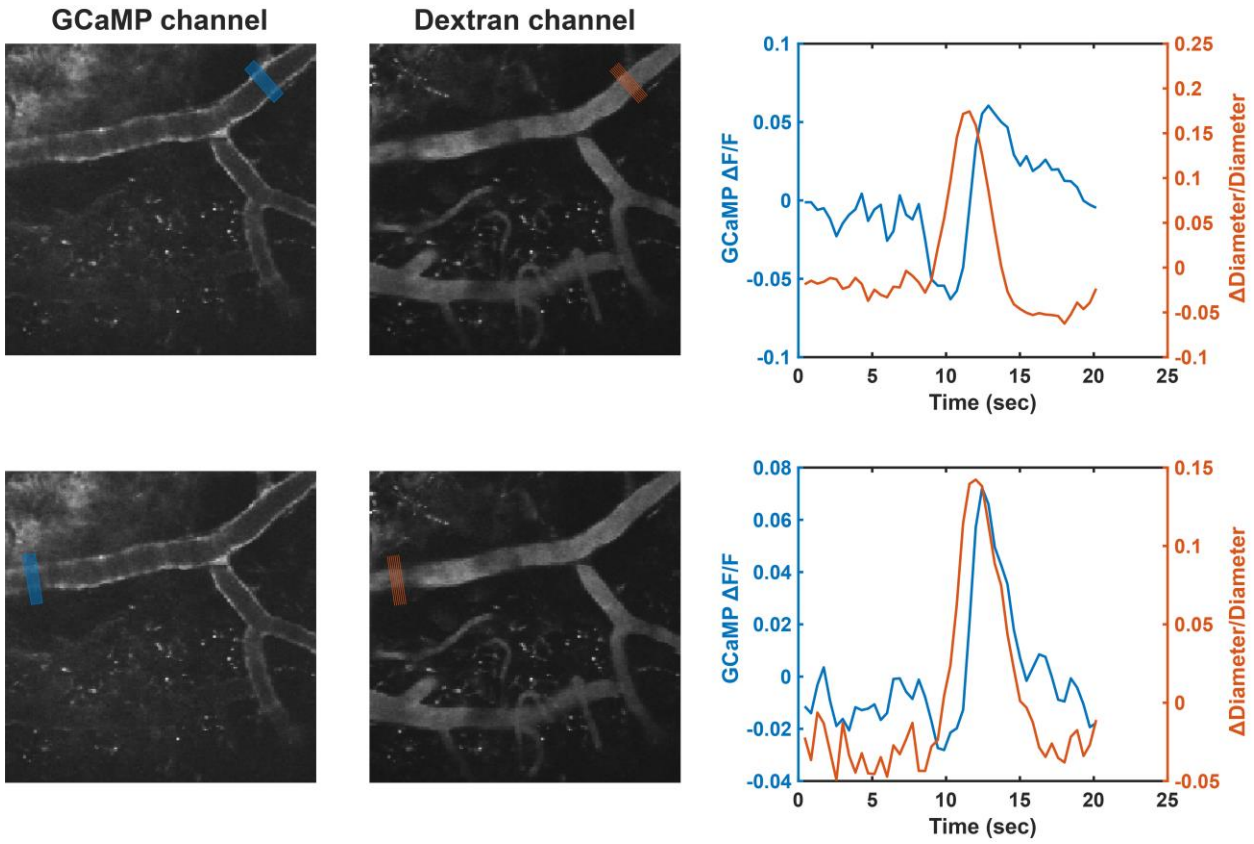

Supplementary figure 4: Simultaneous measurements of calcium signal with a calcium indicator (GCaMP) in the vascular smooth muscle cells (VSMCs) and vessel diameter with plasma labeling during whisker stimulation. *In the left column, the GCaMP image is displayed, with the region of interest (ROI) from which the calcium signal is retrieved shown in blue. In the middle column, the dextran channel is shown, with the ROI where the vessel diameter is calculated in the orange ROI. In the graphs on the right, the retrieved calcium signal and vessel diameter are plotted on the same time-scale, after averaging all 15 stimulation dynamics acquired during the 5-minute timelapse into 1 dynamic. The whisker stimulation starts at 8 seconds. The top row shows the measurement for a more downstream ROI, the bottom row for a more upstream ROI. Note that the distance between the peaks of the orange and blue curves is smaller on the bottom row when compared to the top row.*

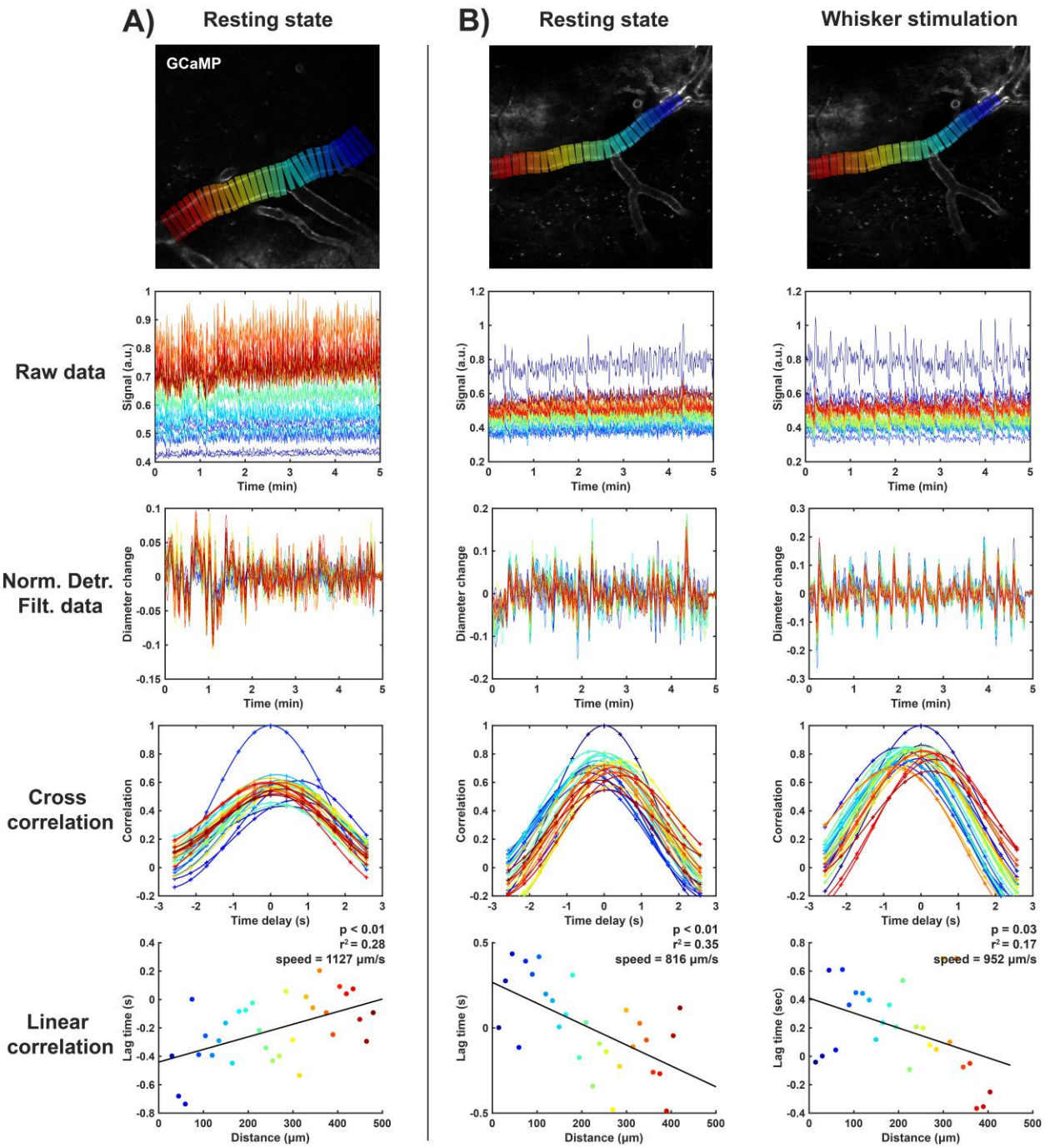

Supplementary figure 5: Examples of the cross-correlation analysis pipeline to measure propagation of calcium concentration changes. *A and B indicate two different datasets. In A, only resting state data was acquired, and in B both resting state and whisker stimulation data (at 0.05 Hz) was acquired. The first row shows the first image of the time-lapse with rainbow-colored regions of interest (ROI) from where the diameter time-profiles were retrieved. The second row shows the raw calcium signal time-profiles; the third row shows normalized, detrended, and low-pass filtered (Norm. Detr. Filt.) time-profiles; the fourth row shows cross-correlation of all the curves in the fourth column with the reference ROI (the first blue ROI); the fifth row shows a linear correlation between the distance along the vessel versus the peaks in the retrieved cross-correlation curves.*

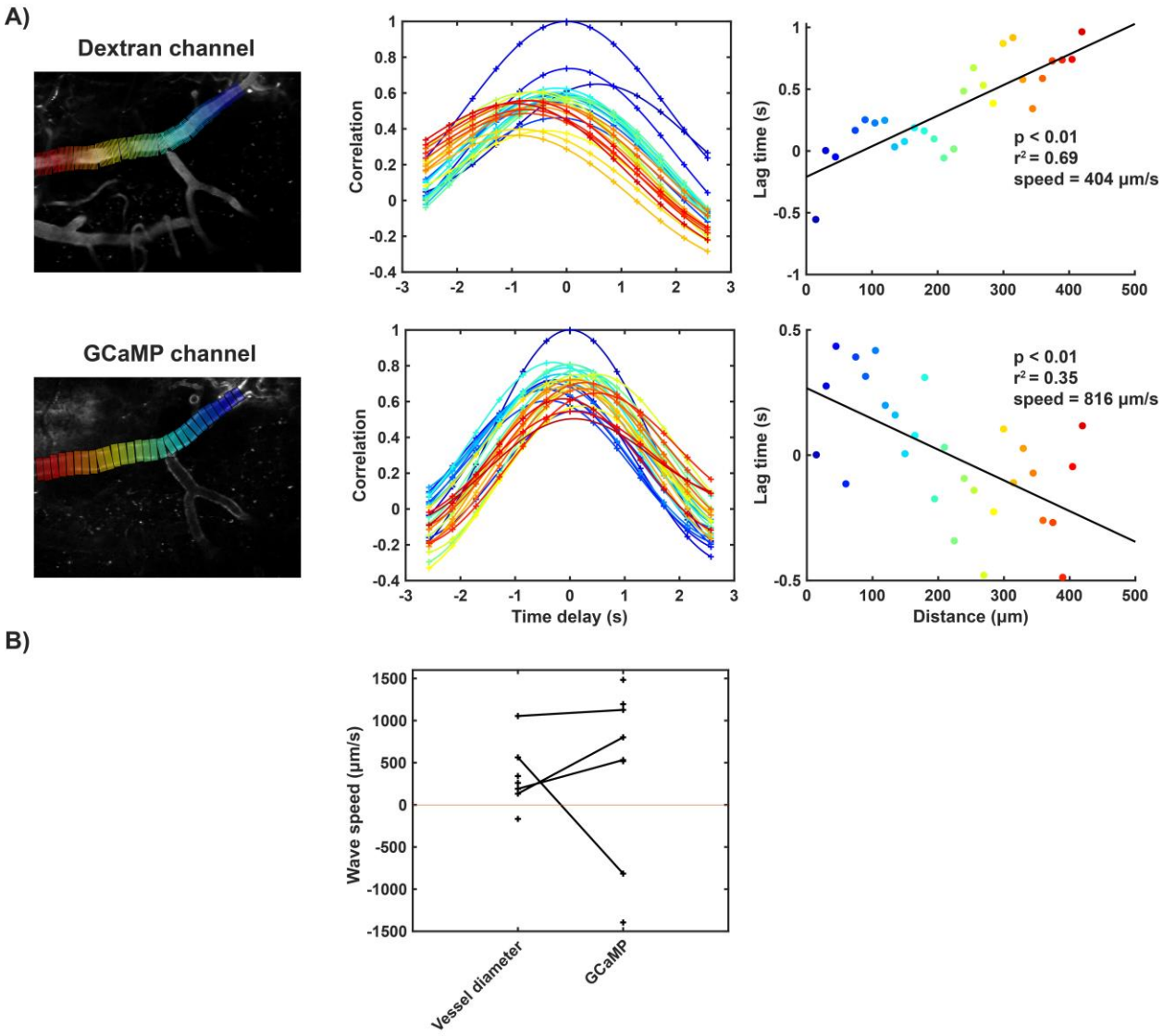

Supplementary figure 6: Simultaneous detection of vessel diameter change propagation and calcium signal propagation with cross-correlation analysis. *A) shows a vessel in which the waves of diameter change and calcium signal move in the opposite direction. The top row shows the vessel channel, the bottom row the calcium indicator (GCaMP) channel. In the left column, the vessel is shown with the ROIs from which the diameter/calcium signal is retrieved. In the middle column, the curves with different colors show the cross-correlation of the signal time-profile from the correspondingly colored ROIs (left image), with the time-profile from the reference ROI (dark blue ROI on the top right of the vessel). In the right column, the distances along the vessel are plotted against the lag time, which is retrieved as the time delay at the peak of the cross-correlation curve of that ROI. Using a linear correlation, the speed of the wave is retrieved. B) shows the wave speeds and directions for all vessels in both imaging channels in cohort 2, where a negative wave speed indicates the wave is moving downstream (with the direction of blood flow). Lines connect wave speed measurements from the two imaging channels acquired in the same vessel. Note that the example shown in A is an exception, as most of the waves travelled either in the same direction, or occurred in isolation.*

Supplementary legends

Supplementary video 1: this video shows an example arteriolar response to 0.12 Hz visual stimulation. Here, all runs within the 5-minute time-lapse (34 runs) are averaged into 1 video.

Supplementary video 2: this is the same video as supplementary video 1, with an additional processing step: every frame from supplementary video 1 is subtracted from the average frame of the same video. Thus, areas where changes occur are highlighted. The first place where there is a change in vessel diameter seems to be on the bottom right of the field of view.